


Article

Crystalline State Hydrogen Bonding of 2-(2-Hydroxybenzylidene)Thiazolo[3,2-*a*]Pyrimidines: A Way to Non-Centrosymmetric Crystals

Artem S. Agarkov ^{1,*}, Igor A. Litvinov ¹, Elina R. Gabitova ², Alexander S. Ovsyannikov ¹ , Pavel V. Dorovatovskii ³, Andrey K. Shiryaev ⁴, Svetlana E. Solovieva ¹ and Igor S. Antipin ¹

¹ Arbuzov Institute of Organic and Physical Chemistry, FRC Kazan Scientific Center, Russian Academy of Sciences, Arbuzova 8, 420088 Kazan, Russia; litvinov@iopc.ru (I.A.L.); osaalex2007@rambler.ru (A.S.O.); evgersol@yandex.ru (S.E.S.); iantipin@yandex.ru (I.S.A.)

² Department of Organic and Medical Chemistry, Kazan Federal University, Kremlevskaya 18, 420008 Kazan, Russia; elina81100@gmail.com

³ National Research Center "Kurchatov Institute", Akademika Kurchatova 1, 123182 Moscow, Russia; paulgemini@mail.ru

⁴ Samara State Technical University, Molodogvardeyskaya 244, 443100 Samara, Russia; shiryaev.ak@samgtu.ru

* Correspondence: artem.agarkov.95.chem@mail.ru

Abstract: Thiazolopyrimidines are attractive to medical chemists as new antitumor agents due to their high inhibiting activity towards the tumor cells replication process and easy modification of their structure by varying of the number and nature of substituents. The presence of asymmetric C5 carbon atoms requires the development of racemic mixture separation procedures for these heterocycles. One of the more effective ways is the crystallization of a racemic compound as a conglomerate. A prerequisite for such separation is the formation of non-centrosymmetric crystals presenting Sohncke space groups. For the construction of chiral supramolecular ensembles in a crystalline state, hydrogen bonds were chosen as supramolecular synthons. In this context, salicylic derivatives at the C2 atom of thiazolopyrimidines were synthesized. The crystal structures of the obtained compounds were established by SCXRD. The regularities of the solvent's influence on the crystal packaging were revealed. The conditions for the preparation of crystals with the chiral space group due to intermolecular hydrogen bonds were discovered.

Keywords: thiazolo[3,2-*a*]pyrimidines; solid state structure; hydrogen bonds; non-centrosymmetric crystals



Citation: Agarkov, A.S.; Litvinov, I.A.; Gabitova, E.R.; Ovsyannikov, A.S.; Dorovatovskii, P.V.; Shiryaev, A.K.; Solovieva, S.E.; Antipin, I.S. Crystalline State Hydrogen Bonding of 2-(2-Hydroxybenzylidene)Thiazolo[3,2-*a*]Pyrimidines: A Way to Non-Centrosymmetric Crystals. *Crystals* **2022**, *12*, 494. <https://doi.org/10.3390/cryst12040494>

Academic Editor: Maija Nissinen

Received: 28 February 2022

Accepted: 31 March 2022

Published: 2 April 2022

Publisher's Note: MDPI stays neutral with regard to jurisdictional claims in published maps and institutional affiliations.



Copyright: © 2022 by the authors. Licensee MDPI, Basel, Switzerland. This article is an open access article distributed under the terms and conditions of the Creative Commons Attribution (CC BY) license (<https://creativecommons.org/licenses/by/4.0/>).

1. Introduction

In the 21st century, cancer ranks first among noncommunicable diseases (NCDs) that have a significant impact on extending of the human life [1]. In this respect, it is still highly challenging to develop new medicaments able to act against a wide variety of cancers and suppress a large range of pathogens. The determination of the structure of such molecules, especially in the crystalline phase, plays an important role in the study of conformational and supramolecular behavior of such species that eventually can afford the development of new synthetic strategies in rational design of such type of compounds aimed to improve their biological activity [2].

In recent years, thiazolopyrimidines (Figure 1) have attracted growing interest as new antitumor agents due to their high inhibiting activity of the tumor cells replication process [3–7].

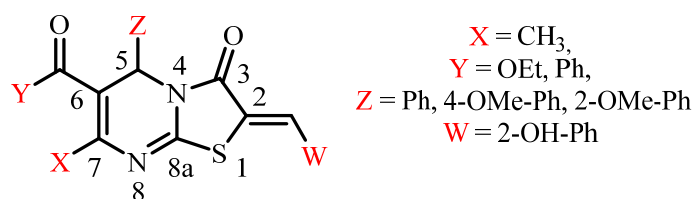


Figure 1. Structure of thiazolo[3,2-*a*]pyrimidines modified by X, Y, Z, and W sites.

Their molecular structure can be easily modified by varying the number and nature of substituents (aromatic, aliphatic, heterocyclic, etc.) at the four main sites (stated as X, Y, Z and W on Figure 1) for adjusting antitumor activity. The methylene group disposed at the second position of the thiazolidine fragment can be considered as one of the most attractive for functionalization because of its high activity in condensation reactions, especially when combined with either aromatic or heterocyclic aldehydes. It was shown that the products obtained by this method can exhibit a wide range of biological activity, i.e., they can act as antitumor agents [8,9] and act as effective growth inhibitors of the Bcl-2 protein that protects the tumor cells from many types of apoptosis [10,11], CDC25 phosphatase that plays a key role in the regulation of the cell reproduction cycle and is usually observed in many types of cancer, casein kinase, and protein kinase [12,13]. Some examples of inhibition of ISPF proteins of *Mycobacterium tuberculosis*, *Plasmodium falciparum*, and *A. thaliana* by such type of compounds were also reported [14].

It is well-known that the majority of biologically active substances used in medicine to treat humans or animals contain chiral centers in their molecular structure, generating optical isomerism. In most cases, only one of the enantiomers has the necessary biological activity [15–17]. The presence of another chiral antipode in the medicament composition may cause or enhance some side effects or even harm the health of a recipient. Thus, the development of separation methods for racemic mixtures of chiral molecules in order to obtain a pure enantiomer form is of great importance [18–20].

Due to the presence of an asymmetric carbon atom in the C5 position, thiazolopyrimidines can exist in both R- and S-enantiomeric forms. (Figure 2).

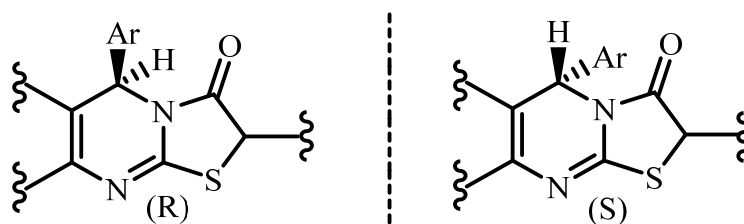
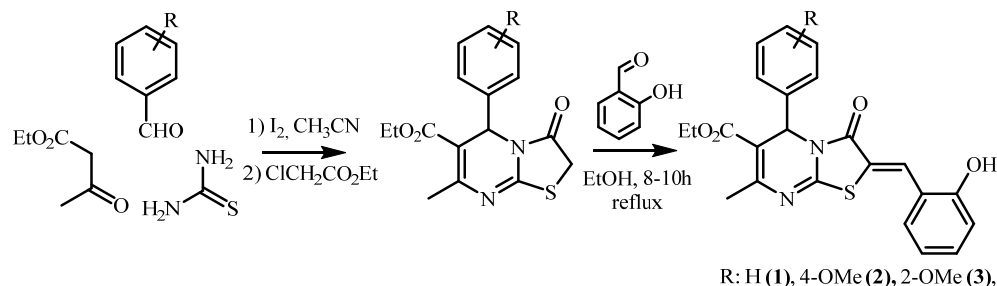


Figure 2. R- and S-enantiomeric forms of thiazolo[3,2-*a*]pyrimidine derivatives.

Some examples of thiazolo[3,2-*a*]pyrimidine derivatives bearing 2-arylidene groups have been already encountered in the literature [14,21–41]. The X-ray diffraction analysis of these compounds revealed that all the obtained structures present a racemic mixture (centrosymmetric crystals). Only one attempt to separate enantiomers by the HPLC method on the chiral stationary phase was reported [14]. It was found that the obtained enantiopure compounds were stable individual substances for more than one week at room temperature. The chiral seeded crystallization, so-called entrainment crystallization method [42], is one of the efficient procedures to separate racemic mixtures. In order to realize this approach, the experimental conditions for the crystallization of a racemic compound as a conglomerate, i.e., as a mechanical mixture of crystals of individual enantiomers, must be established. A prerequisite for such separation is the attempt to crystallize the racemic compounds in Sohncke space groups.

In this paper, we report synthesis and crystal structures of new 2-arylidene thiazolo[3,2-*a*]pyrimidines derivatives (1–3) (Scheme 1) functionalized by proton-donor/acceptor hydroxyl group in D-fragment (Figure 1). The crystallization from protic/aprotic solvents

such as EtOH or DMSO were also applied in order to control the self-assembly of chiral molecules in the crystal phase. The role of intermolecular H-bonding between thiazolo[3,2-*a*]pyrimidines and co-crystallized solvents molecules at the formation of racemic or homochiral crystalline phases will be discussed.



Scheme 1. Hydroxybenzylidene)thiazolo[3,2-*a*]pyrimidines 1–3.

2. Materials and Methods

2.1. Synthesis and Crystallization

All reagents (Acros Organics (Geel, Belgium), Alfa Aesar (Ward Hill, MA, USA)) were used without further purification. The synthesis of the starting 1,2,3,4-tetrahydropyrimidine-2-thions and thiazolo[3,2-*a*]pyrimidines was carried out according to well-known methods in the literature [43–47]. The preparation of target 2-(2-hydroxybenzylidene)thiazolo[3,2-*a*]pyrimidines 1–3 consists of three stages. The first stage is a three-component Biginelli condensation between appropriate aldehyde (1 mmol) (benzaldehyde, 2-methoxybenzaldehyde, 4-methoxybenzaldehyde), thiourea (1.5 mmol), and acetoacetic ether (1 mmol) in the presence of a catalytic amount of molecular iodine (0.03 mmol) at refluxing in acetonitrile for 10 h. The second stage is the reaction of the obtained 1,2,3,4-tetrahydropyrimidine-2-thions (1 mmol) with ethyl chloroacetate (5 mmol) in solvent-free conditions at 110 °C for 2 h. At the final stage of the presented pathway, thiazolo[3,2-*a*]pyrimidines (1 mmol) reacts with salicylic aldehydes (1 mmol) in the presence of a 1% solution of sodium hydroxide and a catalytic amount of pyrrolidine in ethanol for 10 h.

2.1.1. Synthesis of Ethyl (Z)-2-(2-Hydroxybenzylidene)-7-Methyl-3-Oxo-5-Phenyl-2,3-Dihydro-5H-Thiazolo[3,2-*a*]Pyrimidine-6-Carboxylate, Compound 1

A mixture containing ethyl 7-methyl-3-oxo-5-phenyl-2,3-dihydro-5H-thiazolo[3,2-*a*]pyrimidine-6-carboxylate (0.32 g, 1 mmol), 2 drops of pyrrolidine, and salicylic aldehyde (0.134 g, 1.1 mmol) dissolved in 5 mL ethanol was stirred for 10 h at 80 °C. After 10 min of heating, the solution turned red. The precipitate formed after cooling down the reaction mixture to room temperature; it was then filtered out and washed with ethanol (20 mL). Compound 1: yield 80%, mp 215–218 °C; IR (KBr, cm^{-1}): 3371 (OH), 3299 (OH), 1702 (C=O), 1682 (C=O), 1546, 1159, 1081, 754. MALDI-TOF: 421.2 [M]⁺. ¹H NMR (DMSO-*d*₆, 600 MHz) δ 1.12 (3H, *t*, *J* = 12, CH₃), 2.39 (3H, *s*, CH₃), 3.99–4.09 (2H, *m*, OCH₂), 6.05 (1H, *s*, CH), 6.93–6.97 (2H, *m*, Ar-H), 7.28–7.38 (7H, *m*, Ar-H), 7.96 (1H, *s*, C=CH), 10.58 (1H, *s*, OH). ¹³C NMR (DMSO-*d*₆, 151 MHz) δ 13.8, 22.4, 54.7, 60.2, 108.5, 116.2, 118.2, 119.8, 127.4, 128.5, 128.7, 131.5, 132.6, 137.2, 140.4, 151.3, 156.7, 157.2, 164.5. See supplementary materials (Figures S1–S5).

Slow evaporation of the ethanol solution containing dissolved Compound 1 formed monocrystals suitable for SCXRD after 5 days.

2.1.2. Synthesis of Ethyl (Z)-2-(2-Hydroxybenzylidene)-5-(4-Methoxyphenyl)-7-Methyl-3-Oxo-2,3-Dihydro-5H-Thiazolo[3,2-*a*]Pyrimidine-6-Carboxylate, Compound 2

A mixture containing ethyl 5-(4-methoxyphenyl)-7-methyl-3-oxo-2,3-dihydro-5H-thiazolo[3,2-*a*]pyrimidine-6-carboxylate (0.35 g, 1 mmol), 2 drops of pyrrolidine, and salicylic aldehyde (0.134 g, 1.1 mmol) dissolved in 5 mL ethanol was stirred for 10 h

at 80 °C, leading to a red solution. After removing half of the solvent in a vacuum and cooling the mixture to 0 °C for 12 h, yellow precipitate was formed, filtered out, and washed with ethanol. Compound **2**: yield 76%, mp 242–244 °C; IR (KBr, cm⁻¹): 3412 (OH), 1717 (C=O), 1707 (C=O), 1512, 1157, 762. IR (KBr, cm⁻¹): 3434 (OH), 1709 (C=O), 1600, 1542, 1173, 745. MALDI-TOF: 451.6 [M]⁺. ¹H NMR (DMSO-d₆, 600 MHz) δ 1.13 (3H, *t*, *J* = 12, CH₃), 2.38 (3H, *s*, CH₃), 3.71 (3H, *s*, OCH₃), 3.99–4.08 (2H, *m*, OCH₂), 5.99 (1H, *s*, CH), 6.88–6.96 (4H, *m*, Ar-H), 7.21–7.23 (2H, *m*, Ar-H), 7.29–7.36 (2H, *m*, Ar-H), 7.96 (1H, *s*, C=CH), 10.63 (1H, *br. s*, OH). ¹³C NMR (DMSO-d₆, 151 MHz) δ 14.4, 22.9, 54.8, 55.6, 60.6, 107.3, 112.5, 116.6, 118.8, 120.3, 120.5, 127.7, 128.1, 129.1, 130.4, 131.4, 133.1, 151.1, 156.4, 157.5, 158.0, 165.0, 165.8. See supplementary materials (Figures S6–S11).

Slow evaporation of the ethanol (or DMSO) solution containing dissolved Compound **2** formed monocrystals **2a** and **2b**, respectively, suitable for SCXRD after 5 days.

2.1.3. Synthesis of Ethyl (Z)-2-(2-Hydroxybenzylidene)-5-(2-Methoxyphenyl)-7-Methyl-3-Oxo-2,3-Dihydro-5H-Thiazolo[3,2-*a*]Pyrimidine-6-Carboxylate, Compound **3**

A mixture containing ethyl 5-(2-methoxyphenyl)-7-methyl-3-oxo-2,3-dihydro-5H-thiazolo[3,2-*a*]pyrimidine-6-carboxylate (0.35 g, 1 mmol), 2 drops of pyrrolidine, and salicylic aldehyde (0.134 g, 1.1 mmol) dissolved in 5 mL ethanol was stirred for 10 h at 80 °C, leading to a red solution. After removing half of the solvent in a vacuum and cooling the mixture to 0 °C for 12 h, yellow precipitate was formed, filtered out, and washed with ethanol. Compound **3**: yield 85%, mp 187–190 °C; IR (KBr, cm⁻¹): 3434 (OH), 1709 (C=O), 1600, 1542, 1173, 745. MALDI-TOF: 451.6 [M]⁺. ¹H NMR (DMSO-d₆, 600 MHz) δ 1.14 (3H, *t*, *J* = 12, CH₃), 2.29 (3H, *s*, CH₃), 3.72 (3H, *s*, OCH₃), 3.99–4.04 (2H, *m*, OCH₂), 6.17 (1H, *s*, CH), 6.90–7.01 (4H, *m*, Ar-H), 7.25–7.37 (4H, *m*, Ar-H), 7.89 (1H, *s*, C=CH), 10.51 (1H, *s*, OH). ¹³C NMR (DMSO-d₆, 151 MHz) δ 14.3, 22.7, 53.7, 56.0, 60.6, 107.3, 112.5, 116.6, 118.8, 120.3, 120.5, 127.7, 128.1, 129.1, 130.4, 131.4, 133.1, 151.1, 156.4, 157.5, 158.0, 165.0, 165.8. See supplementary materials (Figures S12–S17).

Slow evaporation of the ethanol solution containing dissolved Compound **3** formed monocrystals suitable for SCXRD after 5 days.

An Ultraflex III TOF/TOF mass spectrometer (Bruker Daltonik GmbH, Bremen, Germany) in linear mode was used to register mass spectra. P-nitroaniline and 2,3-dihydroxybenzoic acid were used as matrices.

NMR experiments were performed on Bruker Avance instruments with an operating frequency of 400, 500, and 600 MHz for shooting ¹H and ¹³C NMR spectra, two-dimensional, and low-temperature experiments. Chemical shifts were determined relative to the signals of residual protons of the CDCl₃ or DMSO-d₆ solvents.

IR spectra in KBr tablets were recorded on a Bruker Vector-22. The melting points of the substances were determined on a BOETIUS heating block with a visual device RNMK 05.

The X-ray diffraction study of the crystals **2a** and **3** was performed at the “Belok/XSA” beamline of the Kurchatov Synchrotron Radiation Source [48,49]. Diffraction patterns were collected using Mardtb goniometer (marXperts GmbH, Werkstraße 3, 22844 Norderstedt, Germany) equipped with Rayonix SX165 CCD (Rayonix LLC, 1880 Oak Ave UNIT 120, Evanston, IL, USA) 2D positional sensitive CCD detector (λ = 0.7450 Å, φ-scanning in 1.0° steps). All data were collected at 100 K.

X-ray diffraction analysis of crystal solvates **1** and **2b** was performed on a Bruker D8 QUEST automatic three-circle diffractometer with a PHOTON III two-dimensional detector and an IμS DIAMOND microfocus X-ray tube (λ[Mo Kα] = 0.71073 Å) at 100 (2) K. Data collection and processing of diffraction data were performed using APEX3 software package.

All structures were solved by the direct method using the SHELXT program [50] and refined by the full-matrix least squares method over F² using the SHELXL program [51]. All calculations were performed in the WinGX software package [52]. The calculation of the geometry of molecules and intermolecular interactions in crystals was carried out using the

PLATON program [53], and the drawings of molecules were done using the ORTEP-3 [52] and MERCURY [54] programs.

Non-hydrogen atoms were refined in the anisotropic approximation. The positions of the hydrogen atoms H(O) were determined using difference Fourier maps, and these atoms were refined isotropically. The remaining hydrogen atoms were placed in geometrically calculated positions and included in the refinement in the “riding” model. The crystal of Compound **2b** is a solvate with DMSO (1:1); crystal **1**-solvate with ethanol (1:1). The crystal of Compound **1** is pseudo-centrosymmetric; it was interpreted in the non-centrosymmetric space group $P2_1$ with two independent molecules **1** and two ethanol molecules. The PLATON program proposes a centrosymmetric space group $P2_1/c$ with one molecule of Compound **1** and an ethanol molecule. An attempt to transfer the structure to a centrosymmetric group did not lead to success. The ethoxycarbonyl substituent and the solvate molecules diverged strongly in the structure. R factors in the centrosymmetric space group cannot be obtained below 18%. In addition, systematic absences in the $h0l$ reflections were not observed. As a result, the structure was refined only in the non-centrosymmetric space group. The absolute structure of crystal **1** was not established due to pseudo-centrosymmetric crystal (racemic twin), and in structure **3**, due to the poor quality of the crystal, the Flack parameter [55] was calculated with a high error, and the absolute structure was not determined. Crystallographic data of structures **1–3** were deposited at the Cambridge Crystallographic Data Center; deposition numbers and the crystallographic data are given in Table 1.

Table 1. Crystallographic data for synthesized Compounds **1–3**.

Compound	1 (from Ethanol)	2a (from Ethanol)	2b (from DMSO)	3 (from Ethanol)
Molecular formula	$C_{23}H_{20}N_2O_4 S, C_2H_6O$	$C_{24}H_{22}N_2O_5S$	$C_{24}H_{22}N_2O_5S, C_2H_6OS$	$C_{24}H_{22}N_2O_5S$
Formula	$C_{25}H_{26}N_2O_5S$	$C_{24}H_{22}N_2O_5S$	$C_{26}H_{28}N_2O_6S_2$	$C_{24}H_{22}N_2O_5S$
Formula Weight	466.54	450.50	528.62	450.50
Crystal System	monoclinic	triclinic	monoclinic	orthorhombic
Space group	$P2_1$	$P-1 (P1bar)$	$P2_1/c$	$P2_12_12_1$
Cell parameters	$a = 11.7398(16) \text{ \AA},$ $b = 21.619(3) \text{ \AA},$ $c = 9.6209(13) \text{ \AA};$ $\beta = 108.231(4)^\circ$	$a = 6.6700(13) \text{ \AA},$ $b = 11.210(2) \text{ \AA},$ $c = 14.630(3) \text{ \AA};$ $\alpha = 77.42(3)^\circ$ $\beta = 77.45(3)^\circ$ $\gamma = 78.96(3)^\circ$	$a = 9.6076(8) \text{ \AA},$ $b = 17.8987(15) \text{ \AA},$ $c = 14.7477(12) \text{ \AA};$ $\beta = 101.158(3)^\circ$	$a = 7.7520(16) \text{ \AA},$ $b = 12.147(2) \text{ \AA},$ $c = 22.309(5) \text{ \AA};$
V [\AA^3]	2319.2(6) \AA^3	1030.1(4) \AA^3	2488.1(4) \AA^3	2100.7(7) \AA^3
Z and Z'	4 and 2	2 and 1	4 and 1	4 and 1
D(calc) [g/cm^3]	1.336	1.452	1.411	1.424 $\text{g}\cdot\text{cm}^{-3}$
λ (\AA)	(MoK α) 0.71073	0.7450	(MoK α) 0.71073	0.7450
μ [mm^{-1}]	0.179 MM^{-1}	0.221 MM^{-1}	0.260 MM^{-1}	0.217 MM^{-1}
F(000)	984	472	1112	944
Theta Min-Max [Deg]	1.9–26.5°	2.0–30.0°	2.2–30.0°	1.9–26.3°
Reflections measured	75,170	19,400	118,981	11,919
Independent reflections	9502	5168	7251	3699
Observed reflections [$I > 2\sigma(I)$]	8409	4893	6494	1821
Goodness of fit	0.997	1.03	1.04	0.986

Table 1. Cont.

Compound	1 (from Ethanol)	2a (from Ethanol)	2b (from DMSO)	3 (from Ethanol)
$R [I > 2\sigma(I)]$	$R1 = 0.0277,$ $wR2 = 0.0702$	$R1 = 0.0353,$ $wR2 = 0.0936$	$R1 = 0.0307,$ $wR2 = 0.0818$	$R1 = 0.0848,$ $wR2 = 0.1582$
R (all reflections)	$R1 = 0.0341,$ $wR2 = 0.0719$	$R1 = 0.0368,$ $wR2 = 0.0951$	$R1 = 0.0352,$ $wR2 = 0.845$	$R1 = 0.1879,$ $wR2 = 0.2041$
Max. and Min. Resd. Dens. [$e/\text{\AA}^{-3}$]	0.216 and $-0.182 e \text{\AA}^{-3}$	0.41 and $-0.24 e \text{\AA}^{-3}$	0.52 и $-0.34 e \text{\AA}^{-3}$	0.32 and $-0.34 e \text{\AA}^{-3}$
Flack parameter	0.48(5) (racemic twin, BASF 0.4785)	-	-	0.4(3)
Depositor numbers in CCDC	2,155,259	2,155,261	2,155,263	2,155,264

3. Results and Discussion

To the best of our knowledge, to date, the crystal structures 7-Methyl-3-oxo-5-phenyl-2,3-dihydro-5H-1,3-thiazolo[3,2-*a*]pyrimidine-6-carboxylates are rather scarcely presented in the literature. In the Cambridge Structural Database [56], there are only 23 structures (Figure 3) containing 7-Methyl-3-oxo-2,3-dihydro-5H-1,3-thiazolo[3,2-*a*]pyrimidine-6-carboxylate fragment [14,21–41].

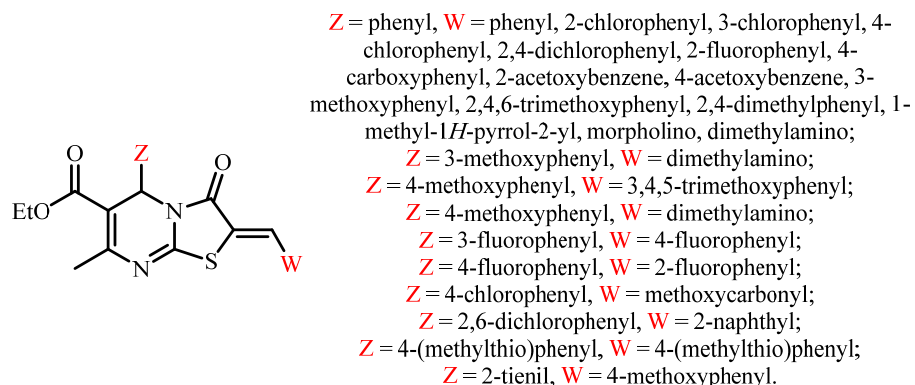


Figure 3. The thiazolo[3,2-*a*]pyrimidines derivatives investigated by single-crystal XRD.

According to single-crystal XRD data analysis, the bicyclic thiazolo[3,2-*a*]pyrimidine fragment is found almost flat in all reported compounds. Six-membered cycle adopts the *sofa* conformation; the sp^3 carbon atom C5 deviates slightly from the plane formed by other five atoms (0.341–0.378 Å). Ethoxycarbonyl and benzylidene substituents are also in the plane of the bicyclic fragment. Apparently, a long electron conjugated system from the ethoxycarbonyl group through the six-membered cycle, the carbonyl group, and the benzylidene substituent of a five-membered cycle is realized in these molecules according to XRD data.

Crystallization of a racemic compound as a conglomerate, i.e., a mechanical mixture of individual enantiomers crystals, is an effective way for the enantiomeric separation from technological and economical perspectives [56]. Through this work, we attempted to determine the experimental conditions for such crystallization of this type of compounds.

Usually, molecules intrinsically are prone to crystallize in symmetric, achiral nonpolar space groups that favor the minimization of dipole moments and close packing in crystal phase. Due to the anisotropic nature and complementarity, hydrogen bonds can be considered as efficient supramolecular synthons [57] for the design of chiral supramolecular assemblies. The construction of the chiral crystals from achiral molecules based on control on self-assembly of chiral 2D hydrogen-bonded layers was described recently [58]. In this aspect, the use of salicylic derivatives at the C2 atom of the bicyclic system seems

a very promising approach to achieve generation of the chiral crystalline phase when interacting with either each other or solvent molecules acting as supplemental H-bond donors or acceptors.

The preparation of four single crystals of new compounds suitable for X-ray diffraction was successfully completed using slow evaporation techniques from ethanol (for **1**, **2a**, **3**) and DMSO (for **2b**). The crystal structures of the obtained crystals were studied using SCXRD, which revealed that all four compounds displayed the conformation behavior of a bicyclic system and the geometric parameters of the molecules similar to the parent compounds. Some selected crystallographic data are presented in Table 1. Aryl fragments in the *Z*-substituent are located in the axial position. The same molecular conformation is observed in all structures reported earlier. Hence, the geometry of molecules will not be discussed below. Particular attention will be focused on the description of crystal packings formed by intermolecular H-bonding.

Compound **1** with phenyl substituent at the C5 atom forms a non-centrosymmetric crystal solvate with ethanol. The asymmetric part consists of two enantiomers (*R* and *S*) of Compound **1** (1A and 1B) and two ethanol molecules. Molecule A is the *S* isomer, and molecule B is the *R* isomer. As was noted in the Experimental section, the *PLATON* proposes to translate the structure into a centrosymmetric space group with one independent molecule. However, an attempt to refine this structure in a centrosymmetric group was not successful. As a result, crystal packing analysis of **1** reveals a non-centrosymmetric system of hydrogen bonds. The hydrogen bonding between Compound **1** and solvate molecules of ethanol leads to the generation of two parallel homochiral chains ($d_{O_{11A}-O_{26A}} = 2.639(3)$ Å, $d_{O_{26A}-N_8} = 2.748(3)$ Å), each composed of only *R*-isomers or *S*-isomers (Figure 4).

In the case of the OMe *para*-substituted derivative **2**, single-crystal XRD revealed the formation of two types of solvates obtained from ethanol **2a** and DMSO **2b**. A unit cell of **2a** presents a centrosymmetric space group and consists of one independent molecule of heterocycle (Figure 5) showing, in this case, no chiral discrimination.

No solvate molecules were found in the crystal of **2a**. The formation of a non-centrosymmetric crystalline solvate with ethanol was not observed. This fact can be associated with steric factor. The H-bonding between two heterocyclic molecules leads to the formation of a centrosymmetric supramolecular dimer crystallized in *triclinic* space group *P*-1 (Figure 5) displaying the O-H . . . O distances equal to 2.696(3) Å and 3.219(2) Å.

Crystals of Compound **2** obtained from DMSO solution also turned out to be centrosymmetric monoclinic and present solvates with one DMSO molecule. They form the 1D-system of intermolecular hydrogen bonds between the hydroxyl group of **2** and the solvent molecule (Figure 6 ($d_{O-O} = 2.664(1)$ Å) and nonclassical CH . . . O H-bonding between methoxy C26-atom and O3-atom carbonyl group of thiazole moiety ($d_{C-O} = 3.077(1)$ Å).

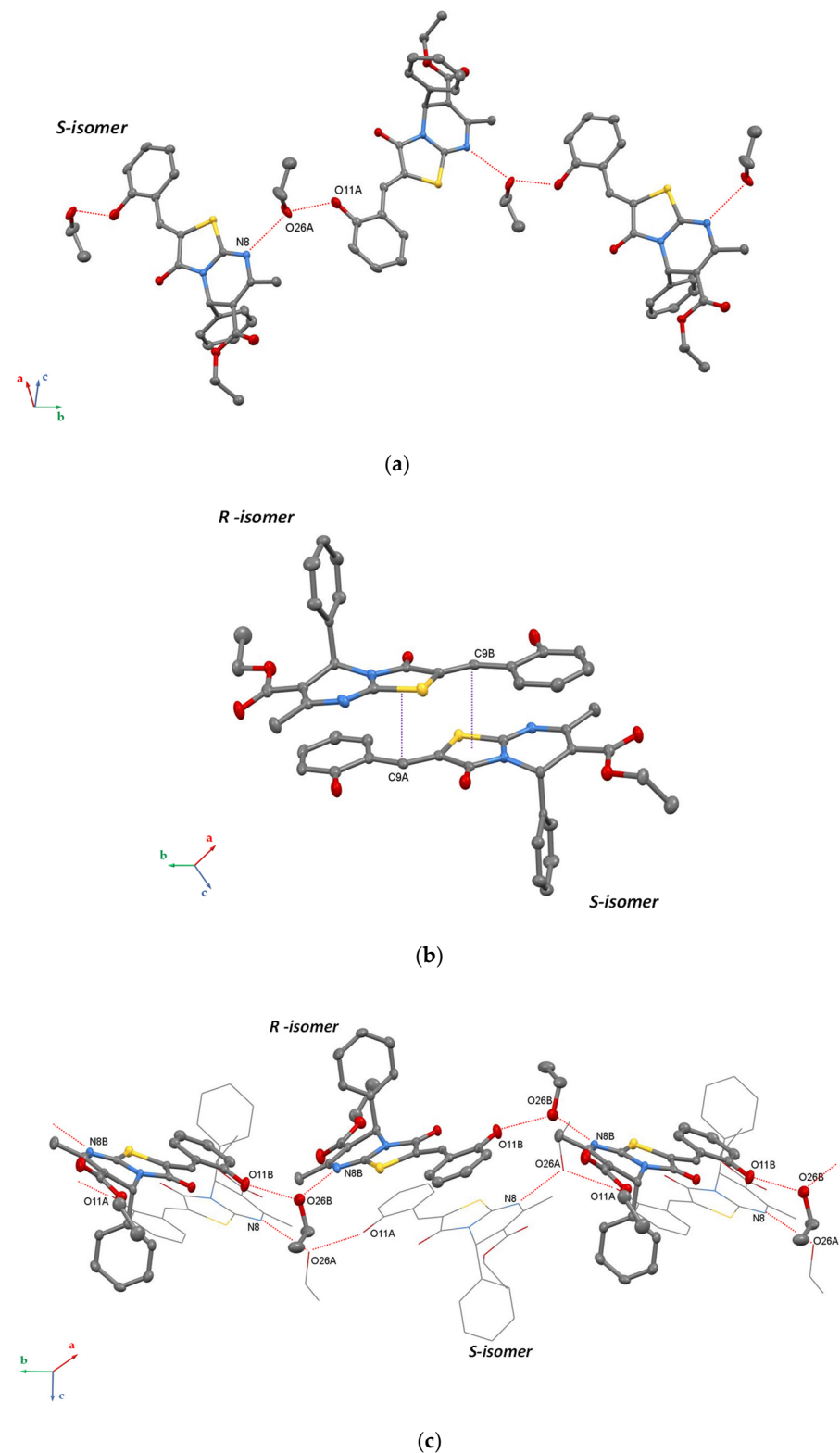


Figure 4. Portion of crystal structure of *rac-1* showing formation of 1D H-bonded zigzag homochiral chain composed of S-isomer (a), π -stacking between R and S isomers ($d_{C9A/C9B-C3Nscntroid} = 3.316 \text{ \AA}$, $\angle = 4.61^\circ$) (b), crystal packing of S and R-isomer based chains (view along *b* axis) (c). Hydrogen bonds and π -stacking are shown by red and violet dotted lines, respectively.

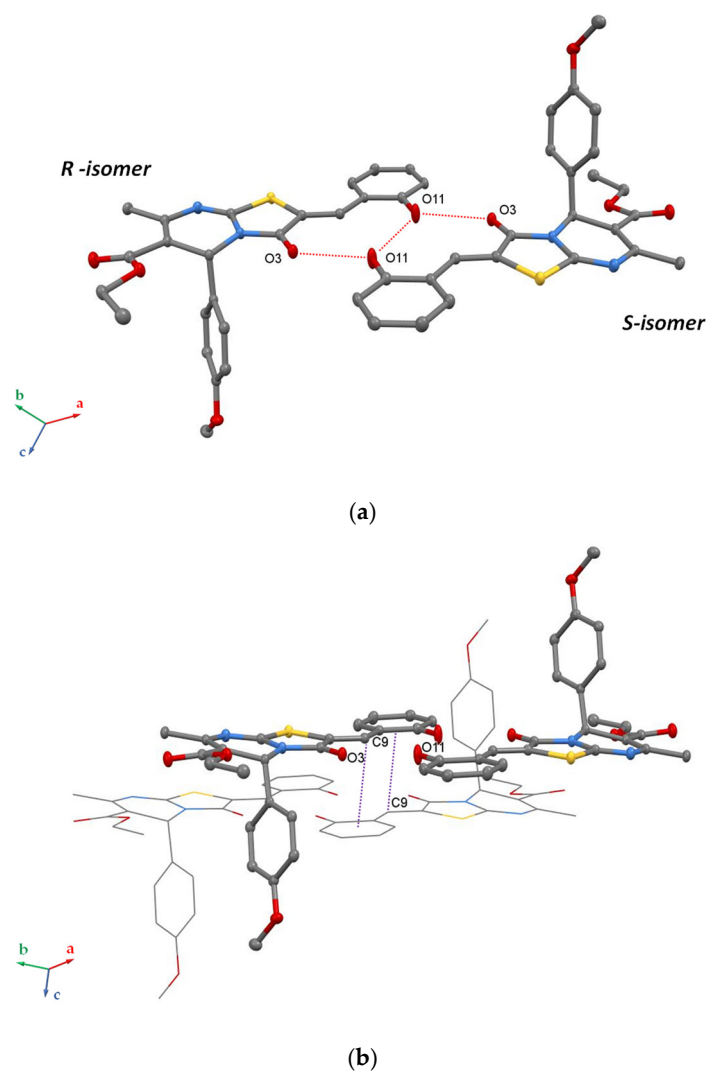


Figure 5. Portion of crystal structure of *rac-2a* showing intermolecular H-bonding between oxygen atoms of *S*- and *R*-isomers leading to supramolecular dimer formation (a), π -stacking between the neighboring dimers within the crystal packing ($d_{C9-C6\text{centroid}} = 3.322 \text{ \AA}$, $\angle = 0^\circ$) (b). Hydrogen bonds and π -stacking are shown by red and violet dotted lines, respectively.

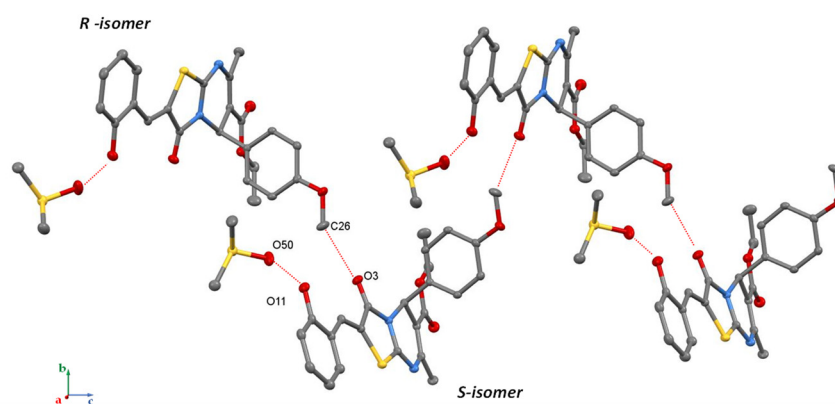


Figure 6. Portion of crystal structure of *rac-2b* showing formation of 1D zigzag chain consisting of *R*- and *S*- isomers and ensured by intermolecular nonclassical CH...O H-bonding between methoxy carbon atom and oxygen of carbonyl group of thiazole moiety (view along *c* axis). Hydrogen bonds are shown in red dotted lines.

Slow crystallization of *ortho*-isomer **3** from ethanol led to the conglomerate formation in the Sohncke space group $P2_12_12_1$ with one independent molecule in the asymmetric part. It should be noted that although crystal **3** is obtained from ethanol solution, it does not contain solvate molecules. Due to the poor diffracting ability of the small crystals of Compound **3**, its crystal structure was established using the synchrotron source of X-rays. It was discovered that the crystal of **3** is composed of only one enantiomer. The system of hydrogen bonds in this crystal is a one-dimensional zigzag chain of molecules. In this case, a different system is implemented than in the previous cases—O11-H... N8 ($d = 2.66(1) \text{ \AA}$) and O11-H... S1 type ($d = 3.132(9) \text{ \AA}$) (Figure 7).

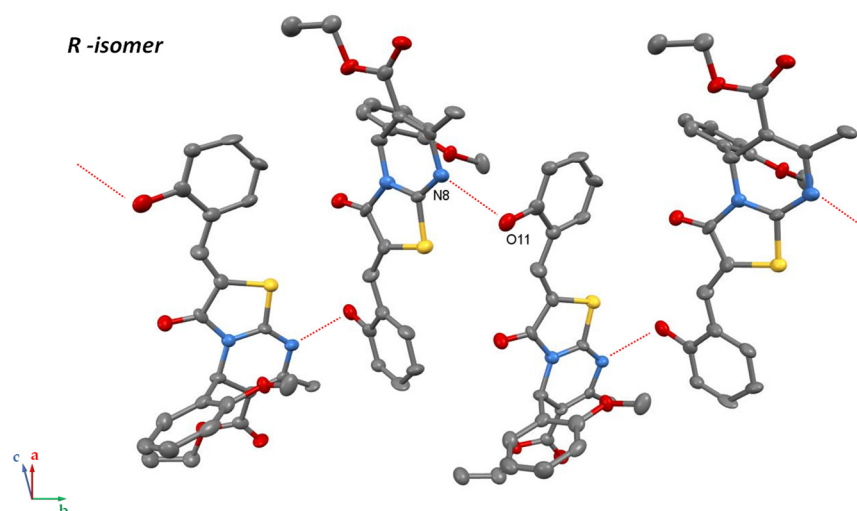


Figure 7. Portion of homochiral crystal structure of **3**, showing formation of 1D H-bonded zigzag chain composed of only R-isomer molecules (view along the *b* axis). Hydrogen bonds are shown in red dotted lines.

In addition, one may notice that the formation of observed H-bonded supramolecular architectures in the studied crystal structures of obtained thiazolo[3,2-*a*]pyrimidines can also be related with OMe group position in the *Z*-substituent, leading to a change in electron density distribution within the molecule. However, in this case, the OMe-group can be considered as a weak H-donor, for which interaction with strong H-acceptors such as an oxygen atom of a carbonyl fragment does not play a dominant role in the formation of the crystal packing where the OH groups are involved in the formation of infinite crystalline structure.

4. Conclusions

In this work, new derivatives of 2-(2-hydroxybenzylidene)thiazolo[3,2-*a*]pyrimidines **1–3** with phenyl and *ortho*-/*para*-anisyl substituents at the C5 atom were obtained. The crystal structures of all synthesized compounds have been established by SCXRD. The regularities of the solvent's influence on the crystal packaging of obtained compounds were studied. The conditions for the preparation of crystals with Sohncke space group due to intermolecular hydrogen bonds were determined. Such a system of hydrogen bonds in the crystal gives the possibility for enantiomer's discrimination of this compound by crystallization condition optimization. It was demonstrated that enantiomeric molecules of thiazolo[3,2-*a*]pyrimidines can be crystallized into racemic or chiral forms. It was shown that hydrogen bonding can be a driving force for the generation of chiral supramolecular assemblies, and crystals in the Sohncke space group $P2_12_12_1$ was obtained. Thus, it could be considered as the first step of enantiomeric separation of 2-(2-hydroxybenzylidene)thiazolo[3,2-*a*]pyrimidines for further investigation of their antitumor activity.

Supplementary Materials: The following supporting information can be downloaded at: <https://www.mdpi.com/article/10.3390/cryst12040494/s1>, Figure S1: ^1H NMR spectrum of compound **1** (DMSO- d_6 , 600 MHz); Figure S2: MALDI TOF spectrum of compound **1** (matrix: p-nitroaniline); Figure S3: IR spectrum of compound **1** (KBr tablet); Figure S4: DSC curves of crystal **1**; Figure S5: HRMS spectrum of compound **1**; Figure S6: ^1H NMR spectrum of compound **2** (DMSO- d_6 , 600 MHz); Figure S7: ^{13}C NMR spectrum of compound **2** (DMSO- d_6 , 600 MHz); Figure S8: MALDI TOF spectrum of compound **2** (matrix: p-nitroaniline); Figure S9: IR spectrum of compound **2** (KBr tablet); Figure S10: DSC curves of crystal **2**; Figure S11: HRMS spectrum of compound **2**; Figure S12: ^1H NMR spectrum of compound **3** (DMSO- d_6 , 600 MHz); Figure S13: ^{13}C NMR spectrum of compound **3** (DMSO- d_6 , 600 MHz); Figure S14: MALDI TOF spectrum of compound **3** (matrix: p-nitroaniline); Figure S15: IR spectrum of compound **3** (KBr tablet); Figure S16: DSC curves of crystal **3a**; Figure S17: HRMS spectrum of compound **3**.

Author Contributions: Conceptualization, I.S.A., A.S.A. and S.E.S.; methodology, A.S.O. and I.A.L.; validation, A.S.A., I.A.L. and A.S.O.; formal analysis, I.A.L., A.S.O. and P.V.D.; investigation, E.R.G., P.V.D., A.S.A. and I.A.L.; resources P.V.D. and I.A.L.; data curation, A.S.A., I.S.A., S.E.S. and A.K.S.; writing—original draft preparation, A.S.A., I.A.L., A.S.O., I.S.A. and S.E.S.; writing—review and editing, A.S.A., I.A.L., A.S.O., I.S.A. and S.E.S.; visualization, A.S.O. and A.S.A.; supervision, I.S.A. and S.E.S.; project administration, A.S.A., I.S.A. and S.E.S.; funding acquisition, I.S.A. All authors have read and agreed to the published version of the manuscript.

Funding: This research was funded by financial support from government assignment for the Arbuzov Institute of Organic and Physical Chemistry, FRC Kazan Scientific Center, Russian Academy of Sciences (122011800132-5).

Institutional Review Board Statement: Not applicable.

Informed Consent Statement: Not applicable.

Data Availability Statement: Not applicable.

Acknowledgments: The authors are grateful to the Assigned Spectral-Analytical Center of Shared Facilities for Study of Structure, Composition and Properties of Substances and Materials of the Federal Research Center of Kazan Scientific Center of Russian Academy of Sciences (CSF-SAC FRC KSC RAS) for technical support.

Conflicts of Interest: The authors declare no conflict of interest. The funders had no role in the design of the study; in the collection, analyses, or interpretation of data; in the writing of the manuscript, or in the decision to publish the results.

References

1. Beaglehole, R.; Bonita, R.; Horton, R.; Ezzati, M.; Bhala, N.; Amuyunzu-Nyamongo, M.; Mwatsama, M.; Reddy, K.S. Measuring progress on NCDs: One goal and five targets. *Lancet* **2012**, *380*, 1283–1285. [[CrossRef](#)]
2. Herbstein, F.H. *Crystalline Molecular Complexes and Compounds: Structures and Principles*; Oxford University Press: Oxford, UK, 2005; Volume 18.
3. Mayer, T.U.; Kapoor, T.M.; Haggarty, S.J.; King, R.W.; Schreiber, S.L.; Mitchison, T.J. Smart molecule inhibitor of mitotic spindle bipolarity identified in a phenotype-based screen. *Science* **1999**, *286*, 971–974. [[CrossRef](#)] [[PubMed](#)]
4. Keshari, A.K.; Singh, A.K.; Saha, S. Bridgehead nitrogen thiazolo[3,2-*a*]pyrimidine: A privileged structural framework in drug discovery. *Mini Rev. Med. Chem.* **2017**, *17*, 1488–1499. [[CrossRef](#)] [[PubMed](#)]
5. Chen, L.; Jin, Y.; Fu, W.; Xiao, S.; Feng, C.; Fang, B.; Gu, Y.; Li, C.; Zhao, Y.; Liu, Z.; et al. Design, Synthesis, and Structure–Activity Relationship Analysis of Thiazolo[3,2-*a*]pyrimidine Derivatives with Anti-inflammatory Activity in Acute Lung Injury. *ChemMedChem* **2017**, *12*, 1022–1032. [[CrossRef](#)]
6. Kashyap, S.J.; Sharma, P.K.; Garg, V.K.; Dudhe, R.; Kumar, N. Review on synthesis and various biological potential of thiazolopyrimidine derivatives. *J. Adv. Sci. Res.* **2011**, *2*, 18–24.
7. Kajal, A.; Bala, S.; Sharma, N.; Kamboj, S.; Saini, V. Mannich Bases: An Important Pharmacophore in Present Scenario. *Int. J. Med. Chem.* **2014**, *2014*, 69–75.
8. Gali, R.; Banothu, J.; Porika, M.; Velpula, R.; Hnamte, S.; Bavantula, R.; Busi, S. Indolylmethylene benzo[*h*]thiazolo[2,3-*b*]quinazolinones: Synthesis, characterization and evaluation of anticancer and antimicrobial activities. *Bioorg. Med. Chem.* **2014**, *24*, 4239–4242. [[CrossRef](#)]
9. Studzińska, R.; Kołodziejaska, R.; Redka, M.; Modzelewska-Banachiewicz, B.; Augustyńska, B. Lipophilicity study of thiazolo[3,2-*a*]pyrimidine derivatives as potential bioactive agents. *J. Braz. Chem. Soc.* **2016**, *27*, 1587–1593. [[CrossRef](#)]

10. Zhou, B.; Li, X.; Li, Y.; Xu, Y.; Zhang, Z.; Zhou, M.; Wang, R. Discovery and Development of 2H-thiazolo[3,2-*a*]pyrimidine Derivatives as General Inhibitors of Bcl-2 Family Proteins. *ChemMedChem* **2011**, *6*, 904–921. [[CrossRef](#)]
11. Feng, Y.; Ding, X.; Chen, T.; Chen, L.; Liu, F.; Jia, X.; Wang, H. Design, synthesis, and interaction study of quinazoline-2(1H)-thione derivatives as novel potential Bcl-xL inhibitors. *J. Med. Chem.* **2010**, *53*, 3465–3479. [[CrossRef](#)]
12. Kolb, S.; Mondésert, O.; Goddard, M.L.; Jullien, D.; Villoutreix, B.O.; Ducommun, B.; Braud, E. Development of Novel Thiazolopyrimidines as CDC25B Phosphatase Inhibitors. *ChemMedChem*. **2009**, *4*, 633–648. [[CrossRef](#)] [[PubMed](#)]
13. Jin, C.H.; Jun, K.Y.; Lee, E.; Kim, S.; Kwon, Y.; Kim, K.; Na, Y. Ethyl 2-(benzylidene)-7-methyl-3-oxo-2,3-dihydro-5H-thiazolo[3,2-*a*]pyrimidine-6-carboxylate analogues as a new scaffold for protein kinase casein kinase 2 inhibitor. *Bioorganic Med. Chem.* **2014**, *22*, 4553–4565. [[CrossRef](#)] [[PubMed](#)]
14. Geist, J.G.; Lauw, S.; Illarionova, V.; Illarionov, B.; Fischer, M.; Gräwert, T.; Rohdich, F.; Eisenreich, W.; Kaiser, J.; Groll, M.; et al. Thiazolopyrimidine inhibitors of 2-methylerythritol 2,4-cyclodiphosphate synthase (IspF) from *Mycobacterium tuberculosis* and *Plasmodium falciparum*. *ChemMedChem*. **2010**, *5*, 1092–1101. [[CrossRef](#)] [[PubMed](#)]
15. Wang, X.; Zeng, S. Stereoselective metabolic and pharmacokinetic analysis of the chiral active components from herbal medicines. *Curr. Pharm. Anal.* **2010**, *6*, 39–52. [[CrossRef](#)]
16. Jozwiak, K.; Lough, W.J.; Wainer, I.W. *Drug Stereochemistry: Analytical Methods and Pharmacology*, 3rd ed.; CRC Press: Boca Raton, FL, USA, 2012.
17. Sekhon, B.S. Exploiting the power of stereochemistry in drugs: An overview of racemic and enantiopure drugs. *J. Mod. Med. Chem.* **2013**, *1*, 10–36. [[CrossRef](#)]
18. Calcaterra, A.; D’Acquarica, I. The market of chiral drugs: Chiral switches versus de novo enantiomerically pure compounds. *J. Pharm. Biomed. Anal.* **2018**, *147*, 323–340. [[CrossRef](#)]
19. Solano, D.M.; Muñoz Solano, D.; Hoyos, P.; Hernáiz, M.J.; Alcántara, A.R.; Sánchez-Montero, J.M. Industrial biotransformations in the synthesis of building blocks leading to enantiopure drugs. *Bioresour. Technol.* **2012**, *115*, 196–207. [[CrossRef](#)]
20. Zhang, Y.; Wu, D.R.; Wang-Iverson, D.B.; Tymiak, A.A. Enantioselective chromatography in drug discovery. *Drug Discov. Today* **2005**, *10*, 571–577. [[CrossRef](#)]
21. Liu, X.G.; Feng, Y.Q.; Li, X.F.; Liang, Z.P. Ethyl 2-(2, 4-dichlorobenzylidene)-7-methyl-3-oxo-5-phenyl-2, 3-dihydro-5H-thiazolo[3,2-*a*]pyrimidine-6-carboxylate dichloromethane solvate. *Acta Crystallogr. Sect. E Struct. Rep. Online* **2004**, *60*, 344–345. [[CrossRef](#)]
22. Jotani, M.M.; Baldaniya, B.B. (2Z)-Ethyl 2-(4-chlorobenzylidene)-7-methyl-3-oxo-5-phenyl-2, 3-dihydro-5H-1, 3-thiazolo[3,2-*a*]pyrimidine-6-carboxylate. *Acta Crystallogr. Sect. E Struct. Rep. Online* **2006**, *62*, 5871–5873. [[CrossRef](#)]
23. Jotani, M.M.; Baldaniya, B.B.; Jasinski, J.P. Crystal Structure of Ethyl (2Z, 5R)-2-benzylidene-7-methyl-3-oxo-5-phenyl-2, 3-dihydro-5H-[1,3] Thiazolo[3,2-*a*]Pyrimidine-6-carboxylate. *J. Chem. Crystallogr.* **2009**, *39*, 898–901. [[CrossRef](#)]
24. Jotani, M.M.; Baldaniya, B.B. Ethyl 2-[(Z)-3-chlorobenzylidene]-7-methyl-3-oxo-5-phenyl-2, 3-dihydro-5H-1, 3-thiazolo[3,2-*a*]pyrimidine-6-carboxylate. *Acta Crystallogr. Sect. E Struct. Rep. Online* **2008**, *64*, 739. [[CrossRef](#)] [[PubMed](#)]
25. Liu, X.G.; Feng, Y.Q.; Li, X.F.; Gao, B. Ethyl 5-(2, 6-dichlorophenyl)-7-methyl-2-(1-naphthylmethylene)-3-oxo-2, 3-dihydro-5H-thiazolo[3,2-*a*]pyrimidine-6-carboxylate. *Acta Crystallogr. Sect. E Struct. Rep. Online* **2004**, *60*, 464–465. [[CrossRef](#)]
26. Banu, N.A.; Raju, V.B. Ethyl 2-(4-carboxybenzylidene)-7-methyl-3-oxo-5-phenyl-2, 3-dihydro-5H-thiazolo[3,2-*a*]pyrimidine-6-carboxylate-N, N-dimethylformamide. *Acta Crystallogr. Sect. E Struct. Rep. Online* **2012**, *68*, 441. [[CrossRef](#)] [[PubMed](#)]
27. Hou, Z.H.; Zhou, N.B.; He, B.H.; Li, X.F. Ethyl 5-(4-chlorophenyl)-2-[(Z)-(methoxycarbonyl) methylene]-7-methyl-3-oxo-3, 5-dihydro-2H-thiazolo[3, 2-*a*]pyrimidine-6-carboxylate. *Acta Crystallogr. Sect. E Struct. Rep. Online* **2009**, *65*, 375. [[CrossRef](#)]
28. Jotani, M.M.; Baldaniya, B.B.; Tiekink, E.R. Ethyl 2-(2-acetoxybenzylidene)-7-methyl-3-oxo-5-phenyl-2, 3-dihydro-5H-1, 3-thiazolo[3,2-*a*]pyrimidine-6-carboxylate. *Acta Crystallogr. Sect. E Struct. Rep. Online* **2010**, *66*, 762–763. [[CrossRef](#)]
29. Baldaniya, B.B.; Jotani, M.M. Crystal Structure of Ethyl (2Z)-2-(4-acetyloxybenzylidene)-7-methyl-3-oxo-5-phenyl-2, 3-dihydro-5H-[1,3] thiazolo[3,2-*a*]pyrimidine-6-carboxylate. *Anal. Sci. X-ray Struct. Anal. Online* **2008**, *24*, 217–218. [[CrossRef](#)]
30. Hou, Z.H. (2Z)-Ethyl 5-(4-methoxyphenyl)-7-methyl-3-oxo-2-(3, 4, 5-trimethoxybenzylidene)-3, 5-dihydro-2H-thiazolo[3,2-*a*]pyrimidine-6-carboxylate. *Acta Crystallogr. Sect. E Struct. Rep. Online* **2009**, *65*, 235. [[CrossRef](#)]
31. Krishnamurthy, M.S.; Nagarajaiah, H.; Begum, N.S. Crystal structure of ethyl 5-(3-fluorophenyl)-2-[(4-fluorophenyl) methylidene]-7-methyl-3-oxo-2H, 3H, 5H-[1,3] thiazolo[3,2-*a*]pyrimidine-6-carboxylate. *Acta Crystallogr. Sect. E Struct. Rep. Online* **2014**, *70*, 1187–1188. [[CrossRef](#)]
32. Jotani, M.M.; Baldaniya, B.B.; Jasinski, J.P. Ethyl (2Z)-2-(3-methoxybenzylidene)-7-methyl-3-oxo-5-phenyl-2, 3-dihydro-5H-1, 3-thiazolo[3,2-*a*]pyrimidine-6-carboxylate. *Acta Crystallogr. Sect. E Struct. Rep. Online* **2010**, *66*, 599–600. [[CrossRef](#)]
33. Nagarajaiah, H.; Begum, N.S. Structural modifications leading to changes in supramolecular aggregation of thiazolo[3,2-*a*]pyrimidines: Insights into their conformational features. *J. Chem. Sci.* **2014**, *126*, 1347–1356. [[CrossRef](#)]
34. Chen, X.Y.; Wang, H.C.; Zhang, Q.; Song, Z.J.; Zheng, F.Y. (Z)-Ethyl 2-(2, 4-dimethylbenzylidene)-7-methyl-3-oxo-5-phenyl-3, 5-dihydro-2H-thiazolo[3,2-*a*]pyrimidine-6-carboxylate. *Acta Crystallogr. Sect. E Struct. Rep. Online* **2012**, *68*, 127. [[CrossRef](#)] [[PubMed](#)]
35. Hu, J.; Wu, X.X.; Shen, X.Q.; Tang, L.G.; Li, X.K. Ethyl 7-methyl-2-((1-methyl-1H-pyrrol-2-yl) methylene)-3-oxo-5-phenyl-3, 5-dihydro-2H-thiazolo[3,2-*a*]pyrimidine-6-carboxylate. *Acta Crystallogr. Sect. E Struct. Rep. Online* **2012**, *68*, 3099. [[CrossRef](#)] [[PubMed](#)]
36. Fischer, A.; Yathirajan, H.S.; Mithun, A.; Bindya, S.; Narayana, B. Ethyl 7-methyl-2-[4-(methylsulfanyl) benzylidene]-5-[4-(methylsulfanyl) phenyl]-3-oxo-2, 3-dihydro-5H-thiazolo[3,2-*a*]pyrimidine-6-carboxylate. *Acta Crystallogr. Sect. E Struct. Rep. Online* **2007**, *63*, 1224–1225. [[CrossRef](#)]

37. Jotani, M.M.; Baldaniya, B.B. Ethyl (2Z)-2-(2-chlorobenzylidene)-7-methyl-3-oxo-5-phenyl-2, 3-dihydro-5H-1, 3-thiazolo[3,2-*a*]pyrimidine-6-carboxylate. *Acta Crystallogr. Sect. E Struct. Rep. Online* **2007**, *63*, 1937–1939. [[CrossRef](#)]
38. Nagarajiah, H.; Khazi, I.A.M.; Begum, N.S. Synthesis of some new derivatives of thiazolopyrimidines and hydrolysis of its arylidene derivative. *J. Chem. Sci.* **2015**, *127*, 467–479. [[CrossRef](#)]
39. Zhao, C.G.; Hu, J.; Zhang, Y.L.; Zhang, J.; Yang, S.L. Ethyl (Z)-2-(2-fluorobenzylidene)-7-methyl-3-oxo-5-phenyl-3, 5-dihydro-2H-thiazolo[3,2-*a*]pyrimidine-6-carboxylate. *Acta Crystallogr. Sect. E Struct. Rep. Online* **2011**, *67*, 3009. [[CrossRef](#)]
40. Banu, N.A.; Bheema Raju, V. Ethyl 7-methyl-3-oxo-5-phenyl-2-(2, 4, 6-trimethoxybenzylidene)-2, 3-dihydro-5H-thiazolo[3,2-*a*]pyrimidine-6-carboxylate. *Acta Crystallogr. Sect. E Struct. Rep. Online* **2012**, *68*, 1213. [[CrossRef](#)]
41. Krishnamurthy, M.S.; Begum, N.S. Crystal structure of ethyl 2-(2-fluorobenzylidene)-5-(4-fluorophenyl)-7-methyl-3-oxo-2, 3-dihydro-5H-1, 3-thiazolo[3,2-*a*]pyrimidine-6-carboxylate. *Acta Crystallogr. Sect. E Struct. Rep. Online* **2014**, *70*, 1270–1271. [[CrossRef](#)]
42. Bredikhin, A.A.; Bredikhina, Z.A.; Gubaidullin, A.T.; Litvinov, I.A. Crystallization of chiral compounds. 2. Propranolol: Free base and hydrochloride. *Russ. Chem. Bull.* **2003**, *52*, 853–861. [[CrossRef](#)]
43. Lashmanova, E.A.; Rybakov, V.B.; Shiryaev, A.K. Synthesis of adamantylated pyrimidines using the Biginelli reaction. *Synthesis* **2016**, *48*, 3965–3970.
44. Shiryaev, A.K.; Baranovskaya, N.S.; Eremin, M.S. Synthesis of 5H-thiazolo[3,2-*a*]pyrimidines. *Chem. Heterocycl. Compd.* **2012**, *48*, 1662–1667. [[CrossRef](#)]
45. Shiryaev, A.K.; Kolesnikova, N.G.; Kuznetsova, N.M.; Lashmanova, E.A. Alkylation of tetrahydropyrimidine-2-thions with ethyl chloroacetate. *Chem. Heterocycl. Compd.* **2013**, *49*, 1812–1817. [[CrossRef](#)]
46. Lashmanova, E.A.; Kiryashkina, A.I.; Slepukhin, P.A.; Shiryaev, A.K. Oxidation of thiazolo[3,2-*a*]pyrimidin-3 (2H)-ones with DMSO and Lawesson's reagent. *Tetrahedron Lett.* **2018**, *59*, 1099–1103. [[CrossRef](#)]
47. Lashmanova, E.A.; Agarkov, A.S.; Rybakov, V.B.; Shiryaev, A.K. Rearrangement of thiazolo[3,2-*a*]pyrimidines into triazolo [4,3-*a*]pyrimidines induced by C=N bond reduction. *Chem. Heterocycl. Compd.* **2019**, *55*, 1217–1221. [[CrossRef](#)]
48. Lazarenko, V.A.; Dorovatovskii, P.V.; Zubavichus, Y.V.; Burlov, A.S.; Koshchienko, Y.V.; Vlasenko, V.G.; Khrustalev, V.N. High-throughput small-molecule crystallography at the 'Belok' beamline of the Kurchatov synchrotron radiation source: Transition metal complexes with azomethine ligands as a case study. *Crystals* **2017**, *7*, 325. [[CrossRef](#)]
49. Svetogorov, R.D.; Dorovatovskii, P.V.; Lazarenko, V.A. Belok/XSA diffraction beamline for studying crystalline samples at Kurchatov Synchrotron Radiation Source. *Cryst. Res. Technol.* **2020**, *55*, 1900184. [[CrossRef](#)]
50. Sheldrick, G.M. SHELXT—Integrated space-group and crystal-structure determination. *Acta Crystallogr. Sect. A Found. Adv.* **2015**, *71*, 3–8. [[CrossRef](#)]
51. Sheldrick, G.M. Crystal structure refinement with SHELXL. *Acta Crystallogr. Sect. C* **2015**, *71*, 3–8. [[CrossRef](#)]
52. Farrugia, L.J. WinGX and ORTEP for Windows: An update. *J. Appl. Crystallogr.* **2012**, *45*, 849–854. [[CrossRef](#)]
53. Spek, A.L. Structure validation in chemical crystallography. *Acta Crystallogr. Sect. D Biol. Crystallogr.* **2009**, *65*, 148–155. [[CrossRef](#)] [[PubMed](#)]
54. Macrae, C.F.; Edgington, P.R.; McCabe, P.; Pidcock, E.; Shields, G.P.; Taylor, R.; Towler, M.; Streek, J.V.D. Mercury: Visualization and analysis of crystal structures. *J. Appl. Crystallogr.* **2006**, *39*, 453–457. [[CrossRef](#)]
55. Flack, H.D.; Bernardinelli, G. Reporting and evaluating absolute-structure and absolute-configuration determinations. *J. Appl. Crystallogr.* **2000**, *33*, 1143–1148. [[CrossRef](#)]
56. Collet, A.; Brienne, M.J.; Jacques, J. Optical resolution by direct crystallization of enantiomer mixtures. *Chem. Rev.* **1980**, *80*, 215–230. [[CrossRef](#)]
57. Desiraju, G.R. Supramolecular synthons in crystal engineering—A new organic synthesis. *Angew. Chem. Int. Ed. Engl.* **1995**, *34*, 2311–2327. [[CrossRef](#)]
58. Sasaki, T.; Ida, Y.; Hisaki, I.; Tsuzuki, S.; Tohnai, N.; Coquerel, G.; Sato, H.; Miyata, M. Construction of Chiral Polar Crystals from Achiral Molecules by Stacking Control of Hydrogen-Bonded Layers Using Type II Halogen Bonds. *Cryst. Growth Des.* **2016**, *16*, 1626–1635. [[CrossRef](#)]